Hyaluronan Self-Agglomerating Nanoparticles For Non-Small Cell Lung Cancer Targeting

Joo-Eun Kim
Catholic University of Daegu
Young-Joon Park (parkyj64@ajou.ac.kr)
Ajou University https://orcid.org/0000-0001-5239-4548

Research

Keywords: Nanoparticle, Targeting, Hyaluronan, Irinotecan, Stability, NSCLC

Posted Date: September 21st, 2021

DOI: https://doi.org/10.21203/rs.3.rs-889315/v1

Version of Record: A version of this preprint was published at Cancer Nanotechnology on March 9th, 2022. See the published version at https://doi.org/10.1186/s12645-022-00115-0.

Abstract

Background: Research into nano-anticancer agents containing water-soluble drug is limited, and no related nano-based anticancer drugs have been developed. In this study, we aimed to develop irinotecan-loaded self-agglomerating hyaluronan nanoparticles (ISHNs) with a high hydrophilic anticancer drug-loading capacity and tumor cell-targeting capability to selectively adhere to overexpressed CD44 on the surface of tumor cells.

Results: The ISHNs, comprising hyaluronic acid as a targeting moiety, ferric chloride as a binder, and D-glutamic acid as a stabilizer, self-agglomerated via chelating bonding and were lyophilized using a freeze dryer. The particle diameter and zeta potential of the ISHNs were 93.8 ± 4.48 nm and -36.3 ± 0.28 mV, respectively; a relatively narrow size distribution was observed. The drug fixation yield and drug-loading concentration were 58.3% and 1.75 mg/mL, respectively. Affinity studies revealed a 10-fold stronger targeting to H23 (cluster of differentiation 44 [CD44]+) non-small-cell lung cancer cells than A549 (CD44-) cells.

Conclusion: Thus, we developed irinotecan-loaded ISHNs, which comprised irinotecan HCl as a water-soluble anticancer agent, HA as a targeting moiety, FeCl3 as a binder for self-agglomeration, and GA as a stabilizer; HA is a binding material for CD44 on the NSCLC cells. Owing to their ease of manufacture, excellent stability, and CD44-targeting ability, they are a potential nanocarrier for passive and active tumor targeting.

Background

Despite the development of many anticancer drugs, efficient chemotherapy has not been achieved because there is no drug delivery system that can efficiently deliver therapeutic drugs to cancer cells (Cho et al. 2010). The most widely used anticancer drug delivery system is currently the injection of an IV infusion of the drug dissolved into an organic solvent, or into a surfactant for an insoluble or poorly soluble anticancer drug (Cho et al. 2014). These drug delivery systems are known to cause side effects when anticancer drugs are administered to normal cells rather than cancer cells. Furthermore, organic solvents used as excipients for anticancer drugs may cause toxic side effects, or surfactants used as excipients for anticancer drugs may necessitate pretreatment, such as the administration of strong steroids, owing to hypersensitivity (Liebmann et al. 1993). To overcome this problem, a variety of tumor targeting methods, such as a passive or active targeting using nanotechnology or a nanoparticle technology, have been studied (Park et al. 2017). These methods use the EPR effect or targeting moieties on the surface of the nanoparticles to enable selective/specific targeting of tumor cells to minimize adverse effects (Choi et al. 2018).

However, research has been limited to drug delivery systems that encapsulate only poorly soluble drugs in nanoparticles (Kim et al. 2017). In the case of poorly soluble anticancer drugs, it is easy to encapsulate drugs in various nanoparticles, such as PLGA (Son et al. 2017), micelles (Danafar et al. 2018), solid lipid nanoparticles (Gupta et al. 2017), liposomes (Seo et al. 2018), cyclodextrins (Jin et al. 2018), and nanoemulsions (Kim et al. 2017, Kim et al. 2017, Kim et al. 2017) by using the hydrophobic or lipid-friendly characteristics of drugs. These offer the advantages of being easy to research and develop as drug-loaded nanoparticles are not dissolved or easily released in aqueous solution after manufacture (Kim et al. 2017).

In contrast, in the case of hydrophilic/water-soluble anticancer drugs, it is extremely difficult to encapsulate water-soluble drugs in various nanoparticles owing to their hydrophilic nature. Even if the water-soluble anticancer agent is encapsulated in the inner part of nanoparticles, it will be dissolved or released into aqueous solution within a few hours (Kim et al. 2017, Kirtane et al. 2017, Sarisozen et al. 2017). Despite the high demand in the market, research into water-soluble nano-anticancer agents is limited, and no related anticancer drugs have been developed. In this study, we aimed to develop self-agglomerating hyaluronan nanoparticles (SAHNs) with the capability to load hydrophilic and

water-soluble anticancer agents and to target tumor cells. To apply self-agglomerating nanoparticle technology, this study investigated the specific properties of irinotecan hydrochloride and the specific properties of hyaluronic acid (HA), which is an endogenous substance and a natural, water-soluble carbohydrate found in the human body and ; moreover, the chelating technique (Zhu et al. 2013) of the μ-oxo form was used, which is generated by the addition of trivalent iron ions, such as ferric chloride (Mercê et al. 2002).

In this study, hyaluronan was employed as a drug carrier for tumor targeting, owing to its specific binding to CD44, which is one of the tumor cell receptors. HA is composed of repeating dimer units (N-acetyl-glucosamine and glucuronic acid), and it is a negatively charged linear polysaccharide. HA is distributed widely throughout the epithelial and neural tissues in our body. It has been investigated as a target molecule owing to its unique properties (Karbownik et al. 2013). HA only binds to CD44 (cluster of differentiation 44), which is a biomarker of cell surface that is over-expressed in the tumors tissue. CD44 is not little expressed in normal cells. A new strategy for active tumor targeting is using through the specific binding of CD44 to HA in cancer therapy. Several nanocarrier formulations have been developed in which HA is connected to the nanocarrier particles, such as HA-coated nanoparticles, HA nanogels, and HA-decorated nanoparticles (Liang et al. 2016, Mohtashamian et al. 2017). These HA-nanocarriers have excellent targeting affinities for tumors, but their limited encapsulation of water-soluble drugs is a serious challenge.

Irinotecan, which is a water-soluble anticancer agent, inhibits DNA synthesis through interference with the action of enzymes for DNA replication and transcription that act on topoisomerase I inhibitor. The indications of irinotecan anticancer drugs are mainly for colorectal cancer and lung cancer. The main side effects of irinotecan include problems with hematopoiesis, such as leukocyte depletion of approximately 80–90% and platelet reduction of 15–30%. To prevent hematopoiesis and the reduction of drug efficacy, our study group iron ion-synthesized nanoparticles containing HA and irinotecan. To fabricate hyaluronan self-agglomerating nanoparticles for tumor targeting in the absence of organic solvents, chemical conjugates, and surfactants, we studied nanoparticles by using trivalent transition metal ions. In particular, self-agglomerating nanoparticle formation technology using ionic bonds (Mercê et al. 2002) can be readily applied to mass production and used immediately in the pharmaceutical industry; thus, it is possible to specifically target drugs to cancer cells. Therefore, it is possible to improve the safety and efficacy of existing water-soluble anticancer drugs (e.g., increase in efficacy, decrease in side effects, and improvements in administration method) and to continuously expand into the market.

This work describes the investigation of the preparation method, characterization of the prepared particles, and the cancer-cell targeting ability of ISHNs encapsulating irinotecan, as a model water-soluble anticancer drug. Specifically, this work aimed to investigate specific strategies to load irinotecan, a model water-soluble anticancer agent, into ISHNs by studying the attachment of the nanoparticle core through electrostatic interaction and the chelation method between the negatively charged carboxyl group of irinotecan and trivalent transition metallic ions.

The ultimate conclusions of this study were: 1) hyaluronan self-agglomerating nanoparticles were prepared to specifically bind to CD44 and target cancer cells; and 2) irinotecan was also self-agglomerated with HA.

Materials And Methods

Materials

Injectable grade sodium hyaluronate (Na-HA) was provided by Bioiberica Co., Ltd. (Barcelona, Spain) and Kibun Food Chemifa Co., Ltd. (Kamogawa, Japan), with molecular weights of approximately 0.5, 0.8, 0.95, 1.5, and 3.6 MDa. Irinotecan hydrochloride of sterilized injectable grade was purchased from Liangyugang Jari Pharmaceutical Co., Ltd. (Shanghai, China). Unites States Pharmacopeia (USP) irinotecan hydrochloride RS was purchased from the United

States Pharmacopeial Convention Inc. (Rockville, MD, USA). Ferric chloride ($FeCl_3$) anhydrous, D-glutamic acid, and phosphate buffer were purchased from Sigma-Aldrich Chemical Co., Ltd. (St. Louis, MO, USA). Ethanol (99.9%), phosphoric acid, and hydrochloric acid was purchased from Duksan Chemical Co., Ltd. (Gyeonggi, Korea). Methanol (99.9%), HPLC-grade acetonitrile, and 0.22 μm membrane filters were purchased from Merck Millipore (Billerica, MA, USA). Camptosar® (irinotecan hydrochloride injection) were purchased from Pfizer Inc. (New York, NY, USA). H23 (CD44+)-expressing human non-small cell lung cancer (NSCLC) cell lines and A549 (CD44-)-expressing human NSCLC cell lines were acquired from the Korean Cell Library Bank(KCBL) and the American Type Culture Collection(ATCC) (Manassas, VA, USA).

Heat-inactivated fetal bovine serum (FBS), N-2-hydroxyethylpiperazine-N-2-ethanesulfonic acid (HEPES), RPMI 1640 cell culture medium (Waymouth), streptomycin, and penicillin were purchased from Gibco Technologies, Inc. (Big cabin, OK, USA). All the chemicals were of reagent grade and were used without further purification.

Preparation of SAHNs

The SAHNs comprised ferric chloride, HA, D-glutamic acid, and water for injection. First, the nanoparticles, which were composed of HA and ferric chloride, were selected based on their compatibility and solubilizing capability and used irinotecan hydrochloride as the model hydrophilic anticancer drug. D-Glutamic acid was chosen as the stabilizer owing to its reconstituted stability and stability in aqueous solution. Moreover, these materials are known to have low toxicity, excellent biodegradability, and biocompatibility in other research studies (Liang et al. 2016, Kim et al. 2017, Kim et al. 2017). The quantities of HA, ferric chloride, and glutamic acid in our SHN formulation were 0.1%, 260 μL, and 800 mg, respectively. The SAHNs were prepared by chelating the μ-oxo form via ionic bonding (Mercê et al. 2002). Briefly, for the extraction of only hyaluronan, 12 g sodium HA (molecular weight: 950,000) was dispersed in 3.0 L of a 7:3 mixture of 99.9% ethanol and 0.1 M HCl solution. The resulting dispersion was kept at 25°C in a 3.0 L beaker and mechanically stirred at 400 rpm for 24 h to reach an equilibrium state and filtered a 0.45 μm RC membrane filter. The sodium HA remaining on the filter was washed three times with 99.9% ethanol and dried in a vacuum desiccator to extract only HA. The obtained HA was confirmed by pH measurement from pH 2.6 to 2.8, and analysis using an FT-IR instrument (Brookfield, NJ, USA) to confirm the presence of a salt peak.

To prepare a stabilized solution of 0.1% HA, 15 mg of the HA was added to 15 mL of 0.02 M D-glutamic acid solution made with water for injection. Thereafter, while stirring the stabilized 0.1% HA solution at 250 rpm with a mechanical stirrer, between 140 and 320 μL of 0.05 M ferric chloride solution was added (stirring was continued for 30 min), and then the solution was cooled to 20°C.

To prepare a stabilized 0.3% HA solution, 45 mg of the obtained HA was added to 15 mL of 0.02 M D-glutamic acid solution made with water for injection. Thereafter, while stirring the stabilized 0.3% HA solution at 250 rpm with a mechanical stirrer, 400–520 μL of 0.05 M ferric chloride solution was added (stirring was continued for 30 min), and then the solution was cooled to 20°C. Finally, the two types of prepared SAHN solutions were lyophilized by using a freeze dryer (Virtis lyophilized dryer™, Warminster, PA, USA).

Preparation of irinotecan-loaded self-agglomerating hyaluronan nanoparticles (ISHNs)

The ISHNs comprised ferric chloride, HA, glutamic acid, irinotecan hydrochloride, and water for injection. For the extraction of only hyaluronan, 12 g sodium HA (molecular weight: 950,000) was dispersed in 3.0 L of a 7:3 mixture of 99.9% ethanol and 0.1 M hydrochloride solution. The resulting dispersion was kept at 25°C in a 3.0 L beaker and mechanically stirred at 400 rpm for 24 h to reach an equilibrium state and filtered a 0.45 μm RC membrane filter. The sodium HA remaining on the filter was washed three times with 99.9% ethanol and dried in a vacuum desiccator to

extract only HA. The obtained HA was confirmed by pH measurement from pH 2.6 to 2.8, and analysis using an FT-IR instrument (Brookfield, NJ, USA) to confirm the presence of a salt peak.

To prepare a stabilized mixed solution with irinotecan and HA, 15 mg of the HA and 45 mg irinotecan hydrochloride were added to 15 mL of 0.02 M glutamic acid solution made with water for injection. Thereafter, the mixture was heated to approximately 60°C and stirred until an aqueous solution was obtained and then cooled to 25°C. The pH was adjusted to approximately 5.0 by using 2 N sodium hydroxide. Thereafter, while stirring the stabilized 0.1% HA solution at 200 to 400 rpm with a mechanical stirrer, 200 µL of 0.05 M ferric chloride aqueous solution was added (stirring was continued for about 1 h), and then the solution was cooled to 20°C. Finally, the prepared ISHNs were lyophilized using a freeze dryer (Virtis lyophilized dryer™, Warminster, PA, USA).

Characterization of SAHNs and ISHNs

Zeta potential, particle size, and polydispersity

The physical properties of particle (zeta potential, size, and polydispersity) of the SAHNs and ISHNs was performed at 25°C a laser scattering particle analyzer using dynamic light scattering (DLS) methods (Model : Zetasizer NanoZS™, Malvern, UK). The reconstituted solutions of SAHNs and ISHNs were diluted 10 times with distilled deionized water and samples measurements were performed 25°C, with a minimum of three replicates.

Morphology

The morphology of ISHNs was monitored by using a nanoparticle tracking analysis (NTA) microscope (NanoSight LM10, Malvern panalytical, Amesbury, UK), equipped with a sample chamber with a 640-nm laser and a viton fluoroelastomer O-ring. The NTA was operated in solution state to analyze the samples. The samples were injected in the sample chamber with sterile syringes (BD Discardit II, New Jersey, USA) until the liquid reached the tip of the nozzle. All measurements were performed at room temperature with the live monitoring heat stress measurements.

Stability studies

Solution stability

Turbiscan Lab® (Formulaction, France) was used to determine the physical solution stability of SAHNs and ISHNs in an aqueous solution in this study. Transmission light for a clear liquid was used. These solution samples were prepared in a 20 mL glass vial (a height of 30 mm) for Turbiscan Lab® equipment. The signal value was obtained every 40 µm throughout the sample. The characteristic analysis of the aggregation behavior was monitored by the measurement of backscattered monochromatic light (λ = 880 nm) by using a Turbiscan Lab® (Formulaction, Toulouse, France) in an aqueous system. The samples were placed in cylindrical glass tubes of flat-bottomed (27.5 mm external diameter, 70 mm height) within placed in the instrument and the backscattered light from the solutions, including SAHNs and ISHNs, was measured at 25°C periodically along the length of the tube.

Physicochemical stability

To ascertain the physicochemical stability, the SAHNs and ISHNs were reconstituted with water for injection. The change in particle size and zeta potential was evaluated on the first day of storage, and after 7 and 14 days of storage at 25°C.

Stability dependency on the ratio of metal ions

To ascertain the physicochemical stability dependency on the ratio of the metal ion to HA, SAHNs and ISHNs were prepared by using the methods described below. However, the methods changed only the stoichiometric ratio (HA disaccharide: iron(□) ion [ferric chloride]), the amount of added iron(□) ion to hyaluronic acid was adjusted from 1:0.18 to 1:0.40.

The SAHNs and ISHNs were reconstituted with water for injection to obtain solutions at a concentration of 1.7 mg/mL irinotecan HCl.

Stability dependency on pH

To ascertain the physicochemical stability dependency on the pH value, SAHNs and ISHNs were prepared by using the methods described below. The methods changed only the manufacturing pH between 2.8 to 8.0 by the addition of K_2CO_3.

Stability dependency on HA concentration

To ascertain the physicochemical stability dependency of the concentration of HA, SAHNs and ISHNs were prepared by using the methods described below. The methods changed only the concentration of HA between 0.1% and 0.3 %. The SAHNs and ISHNs were reconstituted with water for injection. The change in particle size and zeta potential was evaluated on the first day of storage, and after 7 and 14 days of storage at 25°C.

Effect of stabilizer

To ascertain the effect of stabilizers on the nanoparticle, SAHNs and ISHNs were prepared by using the methods described below. The methods changed only the concentration of L-glutamic acid from 0.01 M to 0.05 M. Thereafter, the SAHNs and ISHNs were reconstituted with water for injection. The change in particle size and polydispersity index was evaluated on the first day of storage, and after 1, 2, 4, and 7 days of storage at 25°C.

HPLC analysis

The content of irinotecan hydrochloride was assayed by using a HPLC system, which was equipped with a 255 nm detector and a separation module (Waters 1525/5950 series, CA, Singapore and USA). A C_{18} silica column (Waters, 4.6 mm × 250 mm, 5 µm) was used for the analysis, and the temperature was maintained at 40°C. The mobile phase, which consisted of phosphate buffer, methanol, and acetonitrile (59:24:17, v/v), was filtered a 0.22 µm membrane and degassed by using an online N_2 degasser. The diluent solution was prepared by using mobile phase adjusted with diluted hydrochloric acid to achieve a pH of 3.65 ± 0.15. The flow rate was 1.5 mL/min and the injection volume was 15 µL. The tailing factor was not more than 1.5 and the relative standard deviation (RSD) for replicate injections was not more than 2.0%. After accurately weighing 10 mg irinotecan hydrochloride, the assay samples were prepared by dissolution of the sample and then by dilution of the stock with the diluent to obtain concentrations between 0.05 and 1 mg/mL. The standard deviation (SD) of precision and accuracy was < 2%. The calibration curve was rectilinear, with a correlation coefficient of 0.999. Thereafter, the standard solution was dissolved an accurately weighed quantity of USP irinotecan HCl RS in *Diluent* to obtain a solution with an approximately 1 mg/mL. The assay solution was dissolved in an accurately weighed quantity of irinotecan HCl in *Diluent* to obtain a solution with an approximately 1 mg/mL.

Drug-loading efficiency (LE) and encapsulation efficiency (EE) in ISHNs

To evaluate the EE and LE, 2 mL each of the ISHNs was filtered through a 0.22 μm Acro Disk membrane filter (Emflon Membrane® II of Acro Disk 50 Devices, Pall corp., NY, USA) to remove any unencapsulated irinotecan hydrochloride, which was soluble in the water phase. Subsequently, 1 mL of the filtrate (indirect sample) was measured by using the HPLC assay method described below. Then, 0.05 g of the non-filtrate (ISHNs) was centrifuged at 65,000 *g* for about 1 h by using a Beckman TL 100 Ultracentrifuge (Beckman Coulter, CA, USA) to obtain the entrapped irinotecan hydrochloride in the ISHNs. The centrifuged precipitant was dissolved in 0.05 mL acetonitrile and the drug content encapsulated in the ISHNs was subsequently measured by using the HPLC assay method described below.

The amount of irinotecan hydrochloride entrapped in the ISHNs was calculated from the following equations:

EE (%) = (amount of irinotecan hydrochloride encapsulated in ISHNs / amount of feeding irinotecan hydrochloride) × 100

LE (%) = (amount of irinotecan hydrochloride in ISHNs / amount of feeding material and irinotecan hydrochloride) × 100

In vitro release studies

The 21 h *in vitro* release studies of ISHN 1 (manufactured with 0.02 M ferric chloride), ISHN 2 (manufactured with 0.05 M ferric chloride), and Camptosar® (irinotecan hydrochloride injection) were evaluated by using a previously described dialysis method(Cho et al. 2010). Dialysis membranes (Spectra/Por MW 10,000–12,000, CA, USA) were stabilized by immersion in the releasing medium (2% sodium bicarbonate and 1 mM EDTA in 1 L of ddH_2O) for approximately 40 min before use. Subsequently, 2 mL of the reconstituted ISHNs (ISHN 1, 1.72 mg/mL; and ISHN 2, 1.74 mg/mL) was added to the dialysis tubing attached to a paddle of dissolution tester, and the release of irinotecan was determined according to apparatus 2 of the USP dissolution method (paddle method). The release test was performed with 350 mL of the release medium at 50 rpm and 37°C; 1 mL of the released sample was collected at each time point (0.0416, 0.125, 0.25, 0.5, 1, 2, 3, 4, 5, 6, 7, 8, 9, 10, and every hour for up to 21 h). The content of irinotecan in each sample was measured by using the HPLC method described below. The release medium was continuously replenished to maintain a volume of 350 mL. To compare the release patterns, the diluted 3.5 mg/mL Camptosar® (100 mg/5 mL) was placed into the dialysis tubing attached a paddle of dissolution tester and the release of irinotecan hydrochloride was measured by using the same method as described for the irinotecan release measurements.

In vitro cancer cell-targeting studies

To determine the specific cancer cell affinity of SAHNs for CD44, H23 and A549 cells were used as model non-small cell lung cancer(NSCLC) cells. CD44 is highly expressed on the surface of H23 cells, but not on A549 cells (Leung et al. 2010). The cells were cultured in RPMI 1640 medium supplemented with 10% (v/v) FBS, 100 U/mL penicillin, and 0.1 mg/mL streptomycin and exposed to a humidified atmosphere of 5% CO_2 at 37°C. To detect the binding affinity by using a fluorescence method, FITC was conjugated to the SAHNs by using the following method. The FITC-labeled SAHNs were obtained by conjugation to 0.2 mg FITC instead of the irinotecan hydrochloride by using the preparation method for the SAHNs. The unlabeled fluorescent material was removed by using a cassette type dialysis membrane (Pierce, MW cutoff; 2,000). Subsequently, 20 μg/mL FITC-conjugated SAHNs were added to each H23 and A549 cells line (1×10^6 cells), which was then incubated at 37°C for about 4 h. After the incubation, each H23 and A549 cells line were washed 2 times with PBS (pH 7.4), and treated a 0.1% trypsin for about 2 min. H23 and A549 cells were washed thrice with pH 7.4 of PBS supplemented with preservatives (0.2% FBS and 0.02% sodium azide), and then fixed with 400 μL 4% paraformaldehyde for 10 min. To determine the affinity to CD44, the NSCLC cells were treated with FITC-conjugated SAHNs and then analyzed by using cell-related fluorescence at the emission and excitation wavelengths

(λ) of 520 and 488 nm, respectively, by fluorescence-activated cell sorting (FACS) (Beckton-Dickinson FACScalibur, NJ, USA). The cellular uptake and specific binding of SAHNs were visualized by using a confocal microscope (Olympus LSM 510, Tokyo, Japan).

Statistical analysis

The data are expressed as the mean (x) ± SD. The comparison of the mean between groups was conducted using single factor variance analysis and the LSD test was used for pairwise comparison. Differences were considered statistically significant for P values of 0.05. Minitab® software program (Version eighteen, Minitab Inc., PA, USA) software was used for all statistical analyses.

Results And Discussions

Preparation of SAHNs and ISHNs

Table 1. Physicochemical properties of SAHNs. The data are expressed as the mean ± standard deviation (SD, n = 3).

(A) Stoichiometric ratio of trivalent transition metallic ion and hyaluronic acid

0.3% Hyaluronic acid and $FeCl_3$

Volume of 0.05 M Fe^{3+} ion (µL)	Stoichiometric ratio (HA disaccharide : Fe^{3+})	Size (nm)	% SD	PDI	pH value
400	1 : 0.17	542	-	0.416	2.58
420	1 : 0.18	424	-	0.277	2.58
440	1 : 0.19	492	-	0.352	2.57
460	1 : 0.19	479	-	0.306	2.58
480	1 : 0.20	428	-	0.236	2.58
500	1 : 0.21	407	-	0.214	2.57
520	1 : 0.22	392	-	0.217	2.57

0.1% Hyaluronic acid and $FeCl_3$

Volume of 0.05 M Fe^{3+} ion (μL)	Stoichiometric ratio (HA disaccharide : Fe^{3+})	Size (nm)	% SD	PDI	pH value
140	1 : 0.18	142	4.74	0.365	2.93
150	1 : 0.19	130	7.58	0.208	2.92
160	1 : 0.20	97.8	4.28	0.212	2.90
180	1 : 0.23	88.5	3.20	0.176	2.88
200	1 : 0.25	93.9	3.01	0.143	2.86
220	1 : 0.28	101	1.98	0.128	2.84
240	1 : 0.30	110	2.58	0.090	2.82
260	1 : 0.33	120	1.87	0.157	2.80
280	1 : 0.35	122	4.37	0.144	2.78
300	1 : 0.38	137	1.86	0.127	2.77
310	1 : 0.39	177	0.50	0.252	2.77
320	1 : 0.40	233	1.52	0.262	2.76

(B) Characterization of SAHNs at different pH values

pH	Size (nm)	% SD	PDI	Zeta potential (mV)	Zeta potential SD (mV)
2.81	109	1.32	0.066	-30.3	5.84
3.00	112	1.51	0.094	-31.2	7.36
4.10	149	1.06	0.063	-33.9	6.35
5.10	213	1.11	0.035	-35.8	5.35
6.25	247	1.37	0.114	-44.1	5.23
7.20	267	3.63	0.167	-46.6	4.62

The data are expressed as mean ± standard deviation (SD, n = 5).

(C) Characterization of SAHNs by molecular weight of HA

Volume of 0.05M Fe^{3+} ion (μL)	800,000 Da	950,000 Da	1,500,000 Da	3,600,000 Da
150	139 nm	130 nm	163 nm	N.D.
200	112 nm	108 nm	140 nm	N.D.
250	109 nm	120 nm	164 nm	95.2 nm
300	125 nm	137 nm	151 nm	102 nm
350	233 nm	282 nm	144 nm	117 nm

* N.D. (Not detected): The results did not meet the criteria.

The data are expressed as the mean ± standard deviation (SD, n = 3).

(D) Characterization of SAHNs by concentration of the stabilizer L-glutamic acid

Concentration of glutamic acid (M)	Initial		1 day		2 days		4 days		7 days	
	Size*	% SD	Size	% SD	Size	% SD	Size	% SD	Size	% SD
0.00	108.5	3.45	219.8	1.08	232.0	3.13	243.8	5.47	262.3	6.56
0.01	126.3	2.74	146.0	0.84	153.5	1.64	160.8	3.09	166.8	4.89
0.02	147.7	3.28	154.0	1.15	160.0	2.22	161.3	2.20	163.0	2.87
0.03	139.3	1.84	179.4	0.97	190.7	0.64	198.0	1.96	228.8	1.98
0.04	141.3	2.24	183.3	0.10	194.3	1.66	207.3	2.09	211.8	4.28
0.05	180.0	2.67	185.3	1.01	197.0	1.44	238.3	2.19	219.7	4.44

HA is a natural long-chain polymeric compound based on a disaccharide that is a combination of D-glucuronic acid and N-acetyl-D-glucosamine (Kogan et al. 2007). Each disaccharide, as a monomer, contains one carboxylic group that is engaged in a coordinate bond with iron(□) ion (ferric chloride, $FeCl_3$), where the *stoichiometric ratio* indicates the proportion between the disaccharide and iron(III) ions (i.e. *reaction ratio*) (Mercê et al. 2002, Kim et al. 2017).

To investigate the effects of the variations in proportion on the preparation of SAHNs, ferric chloride, supplied as iron(III) ions, was added to 15 mL HA solution, and then experiments were conducted with constant stirring of 250 rpm at ambient temperature for 5 min. The methods changed only the stoichiometric ratio (HA disaccharide: iron(III) ions [ferric chloride]), the amount of added iron(III) ion to hyaluronic acid was adjusted from 1:0.17 to 1:0.40, and the results are showed in Table 1A.

As shown in Table 1A(up), particle size varied with the specific ratio of HA disaccharide: iron(III) ions [ferric chloride]. First, to investigate effects of iron(III) ion input variations, the amount of 0.05 M iron(III) ions placed into 0.3% HA solution was adjusted to 400–520 μL. Up the addition of ≤ 410 μL, or ≥ 480 μL 0.05 M iron(III) ions to the HA solution, it was found that bead and thread-like precipitates were formed. In terms of efficiency, it was found that the most appropriate amount of 0.05 M iron(III) ions was between 420 μL and 470 μL without any bead and thread-like precipitate, and more than 0.05 M iron(III) ions tended to result in a slightly smaller particle size and a slightly lower polydispersity index(PDI) in aqueous systems.

As shown in Table 1C, to ascertain the size dependency on the molecular weight of HA, the SAHNs were prepared by the methods described below. However, its methods changed only the molecular weight of HA from 800,000 to 3,600,000 Da. As shown in Table 1C, the molecular weight of HA did not affect particle size. In further studies, changes in particle size for HA concentration occurred.

As shown in Table 1A(bottom), when between 160 and 280 µL of 0.05 M iron(III) ions were added into 0.1% HA solution, no significant variations in particle size were observed, but the addition of between 200 and 300 µL of 0.05 M iron(III) ions resulted in a relatively low PDI, indicating that nanoparticles of uniform size were formed. In contrast, the addition of 300 µL or more of 0.05 M iron(III) ions resulted in a drastic increase in particle size and PDI, whereas the addition of 150 µL or less of 0.05 M iron(III) ions resulted in a slightly larger particle size, but a drastic increase in PDI, which indicated that irregularly sized nanoparticles were formed.

As shown in Figure 2C, this study aimed to determine the possible influence of variation in HA %(w/v) concentration, HA concentrations of 0.3%, 0.2%, and 0.1% were tested. To ensure a constant *stoichiometric ratio* (HA disaccharide: iron(III) ion = 1:0.19), the volume of added iron(III) ions was adjusted to 146.7, 293.3, and 440 µL, respectively.

The lowest HA concentrations led to significantly smaller particle size, as shown in Figure 2C; we assumed that potentially, the lower HA solution concentration led to relatively lower opportunities for the combined interactions between the HA molecules directly engaged in the generation and growth of particles.

Additionally, to ascertain the physicochemical stability dependency on ionic strength, SAHNs were prepared by the methods described below. The methods changed only the ionic strength by the addition of KOH, NaOH, Na_2CO_3, and K_2CO_3 at a constant pH value of below 4.0. Through this preliminary studies, in general, the binding ability was reduced at high ionic strength, mainly owing to the electrostatic binding between the functional group and metal ion, as well as the higher counter ion condensation. This study also showed that the higher ionic strength typically yielded smaller particle sizes.

To ascertain the physicochemical stability dependency on temperature, the SAHNs were prepared using the methods described below. The methods changed the manufacturing temperature from 25°C to 45°C.

Through this preliminary studies, the reference for comparative observation of nanoparticles behaviors was also measured without any temperature variation at a certain time, with regard to instability of nanoparticles with time. It was found that the higher temperature led to a slightly larger particle size, and when the temperature was returned to 25°C, the size of nanoparticles at the exact time of temperature return was equivalent to that of nanoparticles kept at the same temperature. This indicated that the size of the formed HA-iron complex nanoparticles with the variation of the temperature was reversible.

Characterization of optimal and ISHNs

The structure and morphology of the ISHNs visualized by using NTA are shown in Figure 1. The ISHNs were spherical with a relatively angular surface and displayed a less smooth spherical shape. The particle size was approximately 80 nm to 180 nm, with a maximum of 183 nm.

It was assumed that the self-agglomerating nanoparticles formed by the covalent bonding were the µ-oxo form (Mercê et al. 2002) between $FeCl_3$ and COOH group of hyaluronan and irinotecan hydrochloride.

As shown in Table 2, the mean diameter of particle size and the PDI of the SAHNs, determined by using DLS, were 89.8 ± 3.31 nm and 0.17 ± 0.03, respectively, which represented a narrow size distribution. The zeta potential reflects the

surface charge that is used to confirm nanoparticle stability. Thus, it is also important for the surface characterization of nanoparticles. The zeta potential of the SAHNs was -31.9 ± 0.32 mV and the surface charge was negative. After lyophilization, the physicochemical characteristics (particle size, size distribution, and zeta potential) of the reconstituted SAHNs were similar to those of the SAHNs.

Table 2. Physicochemical properties of optimal SAHNs and ISHNs. The data are expressed as the mean ± SD (n = 3).

	Formulation	Mean diameter (nm)	Polydispersity index (PDI)	Zeta potential (mV)	Encapsulation efficiency (%)[A]	Drug-loading efficiency (%)[B]	Drug content (mg/mL)[C]
Before lyophilization	SAHNs	89.3 ± 3.31	0.17 ± 0.03	-31.9 ± 0.32	-	-	-
	ISHNs	93.8 ± 4.48	0.19 ± 0.02	-36.3 ± 0.28	58.3 ± 0.15	25.1 ± 0.09	1.75 ± 0.11
After lyophilization	SAHNs	87.5 ± 4.09	0.20 ± 0.05	-31.2 ± 0.25	-	-	-
	ISHNs	95.2 ± 5.56	0.21 ± 0.03	-36.6 ± 0.41	57.3 ± 0.08	24.7 ± 0.07	1.72 ± 0.29

[A] Encapsulation efficiency (%) = (amount of irinotecan hydrochloride encapsulated in ISHNs / amount of the feed source of irinotecan hydrochloride) × 100%

[B] Drug loading efficiency (%) = (amount of irinotecan hydrochloride in ISHNs / amount of the feed source and irinotecan hydrochloride) × 100%

[C] Drug content (mg/mL) = (amount of irinotecan hydrochloride in ISHNs / amount of the feeding material and irinotecan hydrochloride in the 15-mL vial)

Abbreviations: SAHNs, self-agglomerating hyaluronan nanoparticles; ISHN, irinotecan-loaded self-agglomerating hyaluronan nanoparticles.

The mean diameter of the particle size and the PDI of the ISHNs, determined by using DLS, were 93.8 ± 4.48 nm and 0.19 ± 0.02, respectively, which represented a narrow size distribution. The zeta potential of the ISHNs was -36.8 ± 0.28 mV and have a negative surface charge; that is, there was a negative mean charge on the hyaluronan present on the outer surface of the SAHNs and ISHNs. The mean particle size of the ISHNs was much larger than that of the SAHNs ($P < 0.05$) owing to the presence of irinotecan. The ISHNs were 5–7 nm larger than the SAHNs.

After lyophilization, the physicochemical characteristics (particle size, size distribution, and zeta potential) of the reconstituted ISHNs were similar to those of the ISHNs of before lyophilization, as shown in Table 2.

It is known that particle size alters the pharmacokinetics through the alteration of tissue distribution and excretion (Maeda et al. 2013). Nanoparticles below <200 nm show increased drug accumulation in tumor cells because of the EPR effect (Fang et al. 2011). In our study, given that the size of the SAHNs and ISHNs was maintained at not more than 110 nm, irinotecan accumulation of tumor cells was anticipated to be relatively high. Both the SAHNs and ISHNs were a rigid angular spherical shape, and as they are nanoparticles of HA, had a negative charge (Table 1A). These data suggested that the mixture core of the ISHNs contained an irinotecan with a hydroxyl group and that the outside was made with HA in the μ-oxo form covalently bound to $FeCl_3$(ferric chloride) in the aqueous phase. That is,

these nanoparticles such as ISHNs played an important role in the targeting of NSCLC cells. Overall, the zeta potential, particle characteristics, and morphology of the SAHNs and ISHNs were very similar, but the slight difference in particle size was presumably due to the inclusion of irinotecan HCl.

As shown in Table 2, the LE and EE of the ISHNs (n=3) were 25.1% ± 0.09% and 58.3% ± 0.15%, respectively. After reconstitution, the EE and LE of the ISHNs (n=3) were 57.3% ± 0.08% and 24.7% ± 0.07%, respectively, and these results were satisfactory reproducible. The yield of drug fixation reached 50% to 60% in ISHNs. The EE was >58.3% and was independent of the irinotecan content (1.75 mg/mL) for all batches of the ISHNs tested. These data suggested that irinotecan was most conjugated in the HA-agglomerated mixture of the SAHNs. During preliminary studies, we determined that the drug content in the ISHNs was >2 mg/mL; however, to maintain stability over time, we used <1.7 mg/mL of irinotecan for these studies.

Stability studies

To investigate effects of the variation in proportions on the preparation of the HA-iron complex nanoparticles, iron(III) ions were added to 15 mL HA solution, and the experiments were conducted with constant stirring rate at ambient temperature and 250 rpm for 5 min. The methods changed only the stoichiometric ratio (HA disaccharide: iron(□) ion [ferric chloride]); the amount of added iron(III) ion to hyaluronic acid was adjusted from 1:0.18 to 1:0.40.

The SAHNs and ISHNs were reconstituted with injection water to obtain solutions at a concentration of 1.7 mg/mL irinotecan hydrochloride.

The results of the stability dependency of ISHNs on the ratio of metal ion was evaluated by their change of size are shown in Figure 2A. The reconstituted ISHNs without stabilizer were physically unstable when stored at 25°C for 14 days. The size of the tested parameters of the nanoparticles (appearance, particle size, and SD) increased when stored at 25°C for 14 days. Overall, they tended to show an increase in size. However, when between 1 : 0.25 to 0.35 of the stoichiometric ratio(HA:$FeCl_3$) were added into 0.1% HA solution, no significant variations in particle size were observed.

The results of the stability dependency of ISHNs on the pH were evaluated by their change in size over 14 days are shown in Figure 2B. Although the particle size was initially determined by pH, there was no change in particle size over time. The reconstituted ISHNs were physically stable in solutions of various pH stored at 25°C for 14 days. As shown in Figure 2B, the nanoparticles showed no increases in the tested parameters (pH, appearance, particle size, and SD) when stored at 25°C for 14 days. Overall, there was no tendency for the parameters to increase.

The results of the stability dependency of ISHNs on the concentration of HA exhibited between 0.1% to 0.3% are shown in Figure 2C were evaluated by their change in size over 14 days. The initial particle size differed depending on the concentration of HA, and was stable at 0.1% HA, but gradually increased over time at concentrations of 0.2% or more. In our previous experiments, we studied the stability dependency on ionic strength and temperature. Although the particle size was initially determined by the ionic strength and temperature, it did not change over time. The reconstituted ISHNs were physically stable in solutions of various ionic strengths when stored at 25°C for 14 days.

The results of the stability analysis for the total height of samples filled in a cylindrical glass cell using Turbiscan Lab® are shown in Figure 3 and represent the solution stability. The results were measured and illustrated as transmission flux (%) because both samples were of low concentration. Accordingly, the results of analysis were presented in the comparison of transmission flux (%) vs. sample height. As shown in Figure 3A, the reconstituted ISHNs without stabilizer were physically unstable in the test of solution when stored at 25°C for 24 h. However, as shown in Figure 3B, the reconstituted ISHNs with glutamic acid as a stabilizer were physically stable in the test of solution when stored at

25°C for 24 h. Through studies of various materials, L-glutamic acid (GA) was adopted as stabilizer; the coordination with unreacted carboxylic groups occurs in the HA chain and prevents any further growth of particles. Thus, the addition of only 0.02 M GA to the ISHNs achieved the optimal results and there was no significant variation in the size parameters at 25°C for 7 days. That is, the adoption of glutamic acid contributed to marked stabilization, but the concentration of glutamic acid did not influence the stability, except for 0.02 M GA (Table 1D). The data in the table show that higher concentrations of added GA led to a large particle size in the initial step. In particular, the application of 0.02 M GA, as shown in Figure 3B, resulted in smaller and more stabilized uniform size of particles.

In vitro drug release studies

The 21 h *in vitro* drug release patterns of ISHN 1 (manufactured with 0.02 M ferric chloride), ISHN 2 (manufactured with 0.05 M ferric chloride), and Camptosar® (irinotecan hydrochloride) in pH 7.0 PBS, as measured using the above mentioned dialysis method, are shown in Figure 4 (Zhao et al. 2012, Yang et al. 2013, Cho et al. 2014). The Camptosar® injection released >90% of irinotecan within 2 h, whereas the ISHNs released <10% after 2 h and approximately 75% after 10 h. The ISHNs made with 0.02 M and 0.05 M $FeCl_3$ resulted in a sustained released pattern in which the irinotecan hydrochloride was continuously released from the hyaluronan self-agglomerated nanocarriers, and displayed significantly different release characteristics than those of the Camptosar® injection. Further, the release pattern of the ISHNs made with 0.05 M $FeCl_3$ was sustained for a longer period than that of the ISHNs made with 0.02 M $FeCl_3$. These indicated that the *in vitro* release of irinotecan hydrochloride was affected by the bonding among hyaluronan, irinotecan, and ferric chloride, determined by the concentration of ferric chloride. We assumed that the ISHNs may circulate and that retention would be higher than for an irinotecan injection into cancer cells for an extended period after administration. Considering the time required for the formulations to reach the cancer cells after administration in the body, a sustained release of the drug would be more advantageous than a rapid-release formulation and offer greater therapeutic benefits (Cho et al. 2014). Therefore, ISHNs may be more efficient for the delivery of drugs via targeted release than Camptosar® injection.

In vitro NSCLC cell-targeting studies

The results of the *in vitro* NSCLC cell targeting for CD44 exhibited by the SAHNs, which was used to evaluate their capability to target cancer cells that generally overexpress CD44(Taurin et al. 2012) are shown in Figure 5. We used two human NSCLC cell lines, H23 ($CD44^+$) cells, which express CD44 on their surface, and A549 ($CD44^-$) cells, which do not express CD44 (Leung et al. 2010).

The results of the *in vitro* NSCLC cell uptake of the SAHNs for CD44 receptor, which was performed to assess the cell-targeting capability of these nanoparticles toward human NSCLC cells that generally overexpress CD44, are shown in Figure 5.

The all samples used for the *in vitro* cell studies were not experimented ISHNs with an irinotecan, because our team could not evaluate the precise cell count as cell death has been observed following the administration of ISHNs containing anticancer agents such as irinotecan hydrochloride in cell-targeting studies.

As a shown in Figure 5(A), the results of the *in vitro* NSCLC cell affinity studies of the SAHNs for CD44 using A549 (CD44-) cells revealed that specific affinity binding was not observed in all the specimens experimented. The *in vitro* NSCLC cell affinity test of the SAHNs in A549 (CD44-) cells showed that the SAHNs had no specific binding to CD44 present on the NSCLC cells. In contrast, the SAHNs showed substantial specific uptake binding to H23 (CD44+) cells

(Figure 5(A), Bottom). SAHNs had a targeting capability to H23 cells 5-fold higher than that of A549 cells that do not have CD44. Therefore, SAHNs containing HA on the outer-surface of the nanoparticles might offer an outstanding drug delivery system for passive and active tumor targeting.

As a shown in Figure 5(B), the images of the *in vitro* NSCLC cellular uptake and specific affinity of the SAHNs in the H23 and A549 cells captured by using confocal microscopy. The pictures are of single sections through the A549 and H23 cells. The left picture panels, which show nuclear cell staining, were obtained from the blue cell channel; the center picture panels, which show the fluorescence of encapsulated FITC were obtained from the green channel; and the right picture panels are merged pictures from the previous two images. Although the images of the SAHN-treated A549 cells did not reveal any specific binding and cellular uptake, the SAHNs-treated H23 cells were displayed outstanding cellular uptake and specific affinity binding. The results has demonstrated the theory behind the ligand-receptor reaction between HA and CD44. As shown in Figure 5, the results from SAHNs were consistent with confocal microscopy and FACS data, which suggested that SAHNs with HA facilitates attachment to CD44-overexpressing cells in human NSCLC cells. The results of the FACS and confocal microscopy support that the cell affinity of SAHNs should be sufficient to result in efficient cell binding and uptake via CD44 in NSCLC cells. Therefore, it was shown that the SAHNs with HA are a remarkable drug delivery system for passive and active tumor targeting.

Conclusion

To achieve high-efficiency agglomerating encapsulation of water-soluble anticancer drugs, such as irinotecan hydrochloride, in nanoparticles, ion-binding of ferric chloride is used. To prepare a drug delivery system that simultaneously satisfies both passive targeting and active targeting only to cancer cells, irinotecan-hyaluronan self-agglomerating nanoparticles were selected. Since the structure of HA has a carboxyl group and irinotecan has a hydroxyl group, we have applied a ferric chloride as the chelating technique of the μ-oxo form. The investigation of the stoichiometric ratio among HA, irinotecan HCl, and iron(III) ions revealed the production of ISHNs with excellent stability at specific stoichiometric ratios. Through the studies of characterization in the ISHNs, we have identified their physicochemical properties and optimized the self-agglomeration to yield hyaluronan nanoparticles with excellent stability.

Thus, we developed irinotecan-loaded ISHNs, which comprised irinotecan HCl as a water-soluble anticancer agent, HA as a targeting moiety, $FeCl_3$ as a binder for self-agglomeration, and GA as a stabilizer; HA is a binding material for CD44 on the NSCLC cells. The ISHNs had a negatively charged surface that was fabricated with hyaluronan itself by a covalent bond using the μ-oxo form among of hyaluronan, irinotecan, and ferric chloride in the aqueous solution to actively target cancer cells. In the results of *in vitro* drug release studies, we proposed that the ISHNs may circulate and be retained for longer than irinotecan injection in the cancer cells for an extended period after administration. The water-soluble anticancer drug-loaded nanoparticles did not dissociate immediately upon administration in the aqueous solution and also improved the stability of the formulation. The *in vitro* cancer cell targeting study of self-agglomerating nanoparticles to CD44 overexpressed human cancer cells was relatively higher than that to CD44 negative cells. The HA-agglomerated nanoparticles provided remarkable targeting capability for NSCLC cells based on the *in vitro* NSCLC cell targeting study. Furthermore, the ISHNs had a stable particle size of approximately 90 nm, with a narrow size distribution, and were loaded with 1.75 mg/mL of irinotecan HCl inside the hyaluronan-agglomerated complex. In conclusion, these ISHNs were easily manufactured, contained a high payload of water-soluble anticancer agent, and displayed excellent stability and the capability to target a water-soluble anticancer agent to tumor cells.

Abbreviations

HA, hyaluronic acid; SAHNs, self-agglomerating hyaluronan nanoparticles; ISHNs, irinotecan-loaded self-agglomerating hyaluronan nanoparticles; SEM, scanning electron microscope; NSCLC, non-small-cell lung cancer;

Declarations

Acknowledgement

Not applicable

Authors' contributions

J.E. designed the experimental protocols, performed the experiments and analyzed the results. J.E. and Y.J. contributed to writing the manuscript. J.E. and Y.J. revised the manuscript. All authors reviewed the final draft of the manuscript. All authors read and approved the final manuscript.

Funding

This work was supported by the National Research Foundation of Korea (NRF) grant funded by the Korean government (NRF-2018R1C1B5045232).

Availability of data and materials

The data will be available if needed.

Ethics approval and consent to participate

Not applicable.

Consent for publication

All authors agree with the publication of this manuscript in this journal.

Competing interests

The authors declare that there is no conflict of interest.

Author details

[1]First author: Department of Pharmaceutical Engineering, Catholic University of Daegu, Hayang-Ro 13-13, Gyeongsan City, Gyeongbuk, Republic of Korea. 38430

[2]Corresponding author: College of Pharmacy. Ajou University, Suwon City, 443-749, Korea

References

Cho, Y.-D. and Y.-J. Park (2010). "Preparation and evaluation of novel fenofibrate-loaded self-microemulsifying drug delivery system (SMEDDS)." Journal of Pharmaceutical Investigation **40**(6): 339-345.

Cho, Y.-D. and Y.-J. Park (2014). "In vitro and in vivo evaluation of a self-microemulsifying drug delivery system for the poorly soluble drug fenofibrate." Archives of pharmacal research **37**(2): 193-203.

Choi, Y. H. and H.-K. Han (2018). "Nanomedicines: current status and future perspectives in aspect of drug delivery and pharmacokinetics." Journal of Pharmaceutical Investigation **48**(1): 43-60.

Danafar, H., et al. (2018). "Polylactide/poly (ethylene glycol)/polylactide triblock copolymer micelles as carrier for delivery of hydrophilic and hydrophobic drugs: a comparison study." Journal of Pharmaceutical Investigation **48**(3): 381-391.

Fang, J., et al. (2011). "The EPR effect: unique features of tumor blood vessels for drug delivery, factors involved, and limitations and augmentation of the effect." Advanced Drug Delivery Reviews **63**(3): 136-151.

Gupta, B., et al. (2017). "Solid matrix-based lipid nanoplatforms as carriers for combinational therapeutics in cancer." Journal of Pharmaceutical Investigation **47**(6): 461-473.

Jin, S.-E., et al. (2018). "Evaluation of nitroglycerin and cyclosporin A sorption to polyvinylchloride-and non-polyvinylchloride-based tubes in administration sets." Journal of Pharmaceutical Investigation **48**(6): 665-672.

Karbownik, M. S. and J. Z. Nowak (2013). "Hyaluronan: towards novel anti-cancer therapeutics." Pharmacological Reports **65**(5): 1056-1074.

Kim, C. H., et al. (2017). "Surface modification of lipid-based nanocarriers for cancer cell-specific drug targeting." Journal of Pharmaceutical Investigation **47**(3): 203-227.

Kim, H. S. and D. Y. Lee (2017). "Photothermal therapy with gold nanoparticles as an anticancer medication." Journal of Pharmaceutical Investigation **47**(1): 19-26.

Kim, J.-E. and Y.-J. Park (2017). "High paclitaxel-loaded and tumor cell-targeting hyaluronan-coated nanoemulsions." Colloids and Surfaces B: Biointerfaces **150**: 362-372.

Kim, J.-E. and Y.-J. Park (2017). "Improved antitumor efficacy of hyaluronic acid-complexed paclitaxel nanoemulsions in treating non-small cell lung cancer." Biomolecules & therapeutics **25**(4): 411.

Kim, J.-E. and Y.-J. Park (2017). "Paclitaxel-loaded hyaluronan solid nanoemulsions for enhanced treatment efficacy in ovarian cancer." International journal of nanomedicine **12**: 645.

Kirtane, A. R., et al. (2017). "Polymer-surfactant nanoparticles for improving oral bioavailability of doxorubicin." Journal of Pharmaceutical Investigation **47**(1): 65-73.

Kogan, G., et al. (2007). "Hyaluronic acid: a natural biopolymer with a broad range of biomedical and industrial applications." Biotechnology letters **29**(1): 17-25.

Leung, E. L.-H., et al. (2010). "Non-small cell lung cancer cells expressing CD44 are enriched for stem cell-like properties." PloS one **5**(11): e14062.

Liang, J., et al. (2016). "Hyaluronan as a therapeutic target in human diseases." Advanced Drug Delivery Reviews **97**: 186-203.

Liebmann, J., et al. (1993). "Cremophor EL, solvent for paclitaxel, and toxicity." The Lancet **342**(8884): 1428.

Maeda, H., et al. (2013). "The EPR effect for macromolecular drug delivery to solid tumors: Improvement of tumor uptake, lowering of systemic toxicity, and distinct tumor imaging in vivo." Advanced Drug Delivery Reviews **65**(1): 71-79.

Mercê, A. L. R., et al. (2002). "Aqueous and solid complexes of iron (III) with hyaluronic acid: potentiometric titrations and infrared spectroscopy studies." Journal of inorganic biochemistry **89**(3-4): 212-218.

Mohtashamian, S. and S. Boddohi (2017). "Nanostructured polysaccharide-based carriers for antimicrobial peptide delivery." Journal of Pharmaceutical Investigation **47**(2): 85-94.

Park, O., et al. (2017). "Recent studies on micro-/nano-sized biomaterials for cancer immunotherapy." Journal of Pharmaceutical Investigation **47**(1): 11-18.

Sarisozen, C., et al. (2017). "Polymers in the co-delivery of siRNA and anticancer drugs to treat multidrug-resistant tumors." Journal of Pharmaceutical Investigation **47**(1): 37-49.

Seo, J., et al. (2018). "Enhanced topical delivery of fish scale collagen employing negatively surface-modified nanoliposome." Journal of Pharmaceutical Investigation **48**(3): 243-250.

Son, G.-H., et al. (2017). "Mechanisms of drug release from advanced drug formulations such as polymeric-based drug-delivery systems and lipid nanoparticles." Journal of Pharmaceutical Investigation **47**(4): 287-296.

Taurin, S., et al. (2012). "Anticancer nanomedicine and tumor vascular permeability; where is the missing link?" Journal of controlled release **164**(3): 265-275.

Yang, X. Y., et al. (2013). "Hyaluronic acid-coated nanostructured lipid carriers for targeting paclitaxel to cancer." Cancer Lett **334**(2): 338-345.

Zhao, P., et al. (2012). "Paclitaxel loaded folic acid targeted nanoparticles of mixed lipid-shell and polymer-core: in vitro and in vivo evaluation." Eur J Pharm Biopharm **81**(2): 248-256.

Zhu, M., et al. (2013). "In situ structural characterization of ferric iron dimers in aqueous solutions: Identification of μ-oxo species." Inorganic Chemistry **52**(12): 6788-6797.

Figures

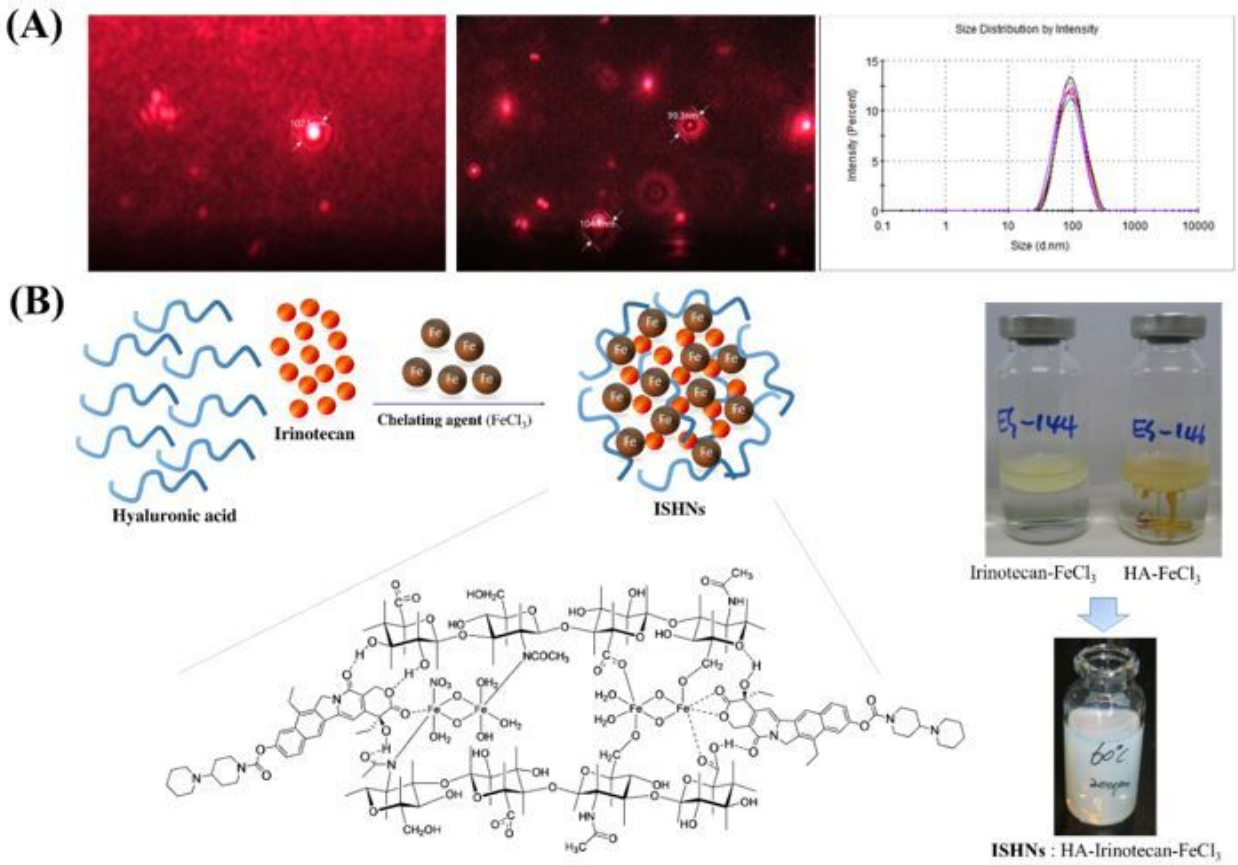

Figure 1

Schematic representation and illustration of the ISHNs structure (B) and SEM image of the ISHNs (A) Note: SEM image scale bar = 1,000nm, Abbreviation: HA, hyaluronic acid; SAHNs, self-agglomerating hyaluronan nanoparticles; ISHNs, irinotecan-loaded self-agglomerating hyaluronan nanoparticles; SEM, scanning electron microscope.

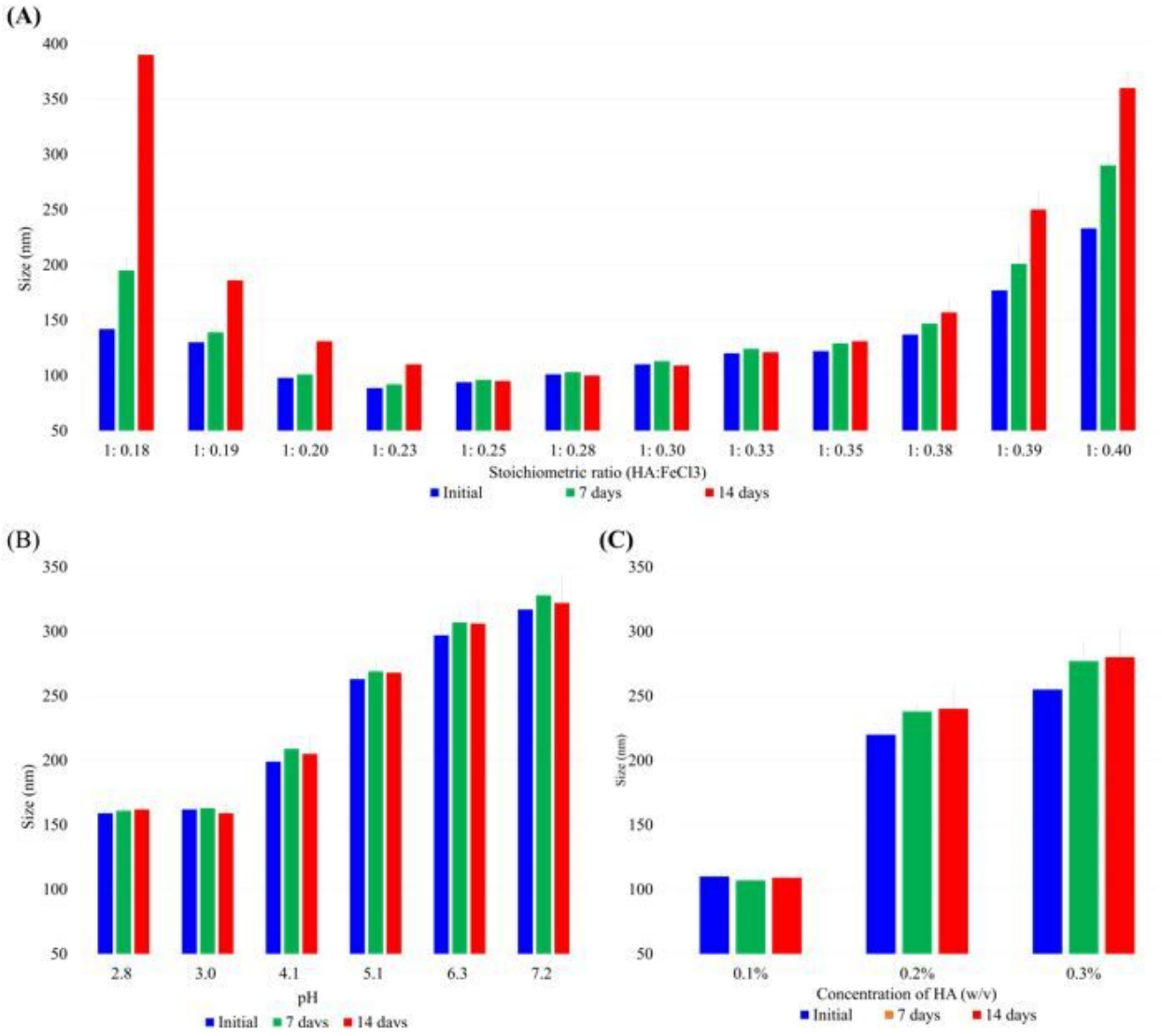

Figure 2

Stability studies Stability dependent in the ratio of metal ion(A), Stability dependency on pH (B), and stability dependency on HA concentration (C), Abbreviation: HA, hyaluronic acid; ISHNs, irinotecan-loaded self-agglomerating hyaluronan nanoparticles

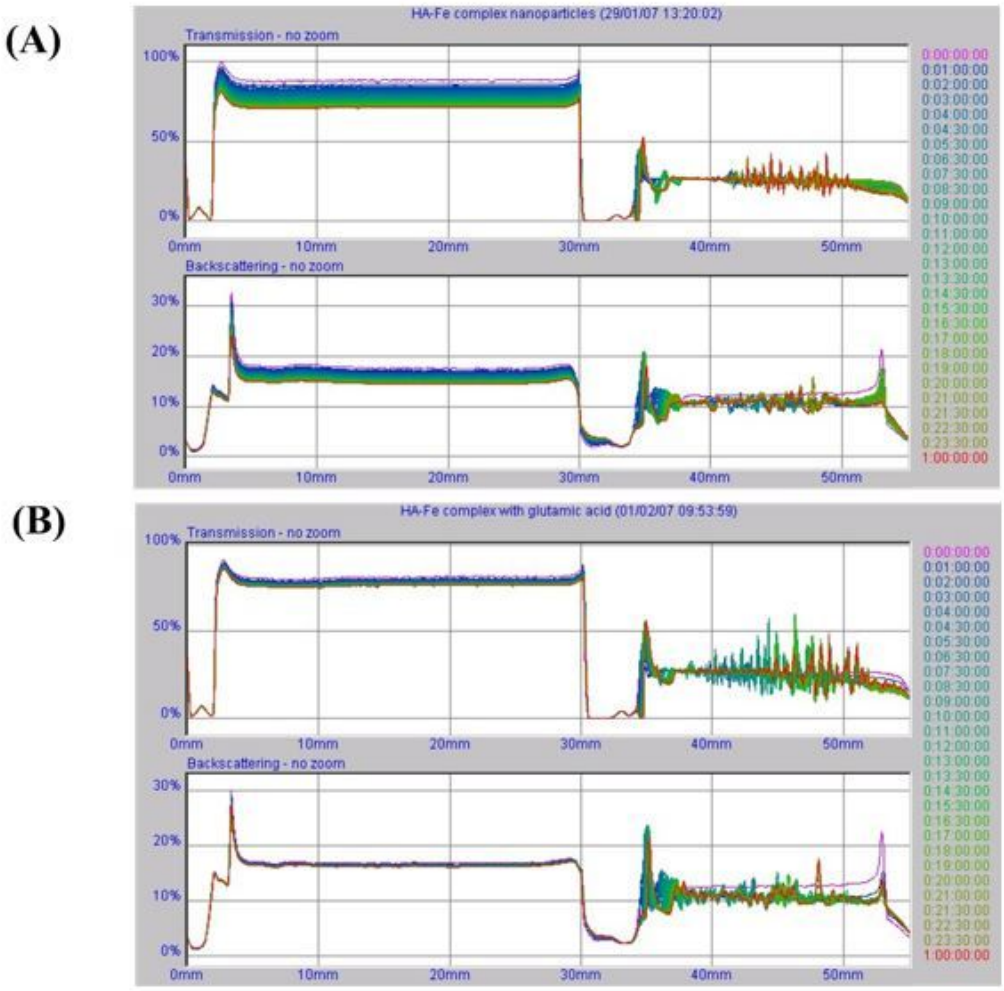

Figure 3

Solution stability of the ISHNs It was performed the results of stability analysis for total height of samples filled in a cylindrical glass cell using Turbiscan Lab® for solution stability, the ISHNs without L-glutamic acid as stabilizer (A), and the ISHNs with L-glutamic acid as stabilizer (B). Abbreviation: HA, hyaluronic acid; ISHNs, irinotecan-loaded self-agglomerating hyaluronan nanoparticles.

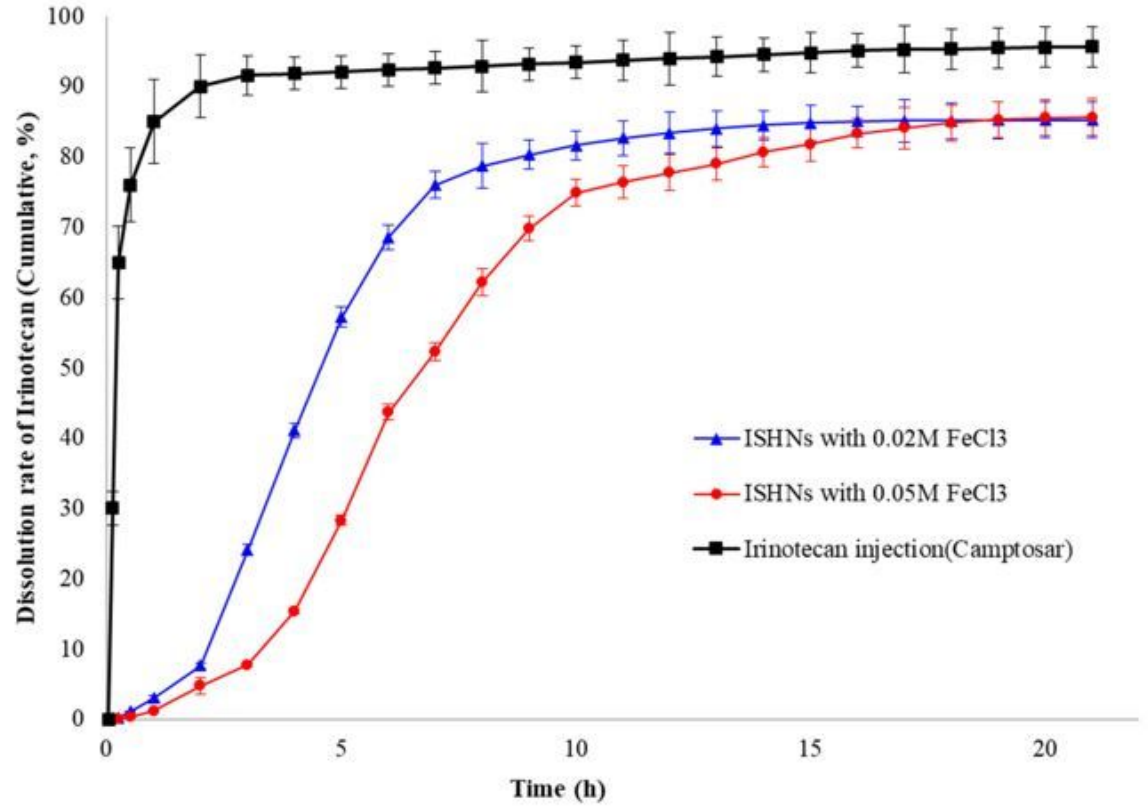

Figure 4

In vitro drug release studies In vitro drug release of the ISHNs and irinotecan injection. Irinotecan hydrochloride release was determined at pH 7.0. The data are expressed as the mean ± SD (n = 3).

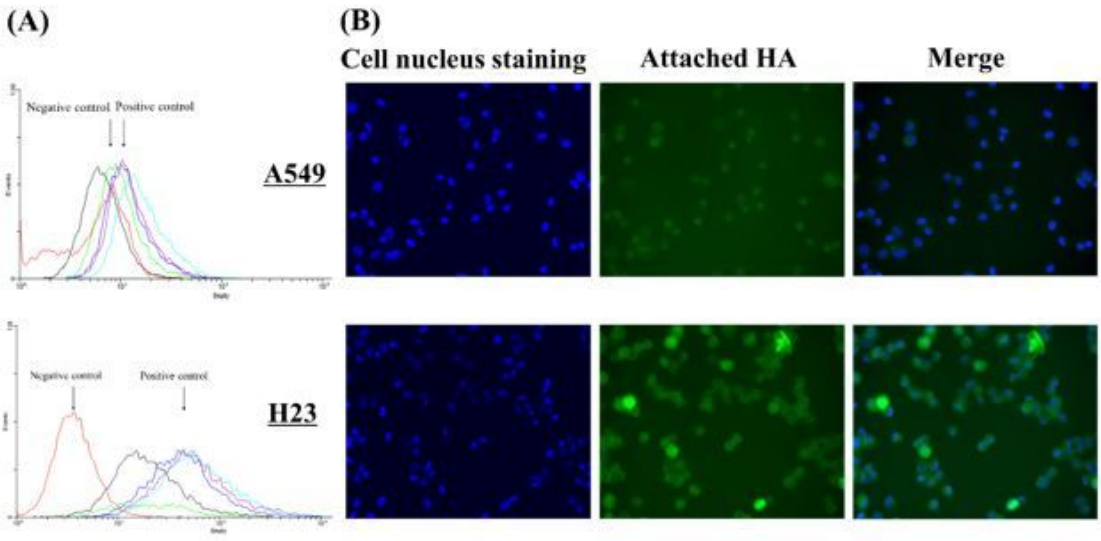

Figure 5

In vitro cancer cell targeting studies of ths SAHNs. FACS was performed in A549 cells and H23 cells of the human non-small cell lung cancer cell lines. FITC-labeled SAHNs were prepared with 0.1 %(w/v) HA (A). Confocal microscopy

images of SHNs in A549 (CD44-negative) and H23 (CD44-positive) cells (B). Abbreviation: HA, hyaluronic acid; SAHNs, self-agglomerating hyaluronan nanoparticles.

Supplementary Files

This is a list of supplementary files associated with this preprint. Click to download.

- Graphicalabstract.tif